Optimization Of CO2 injection using multi-scale reconstruction of compositional transport

Chen, Y.; Voskov, D.; Khait, M.

DOI
10.3997/2214-4609.201802240

Publication date
2018

Document Version
Final published version

Published in
16th European Conference on the Mathematics of Oil Recovery, ECMOR 2018

Tu A1 04

Optimization Of Co2 Injection Using Multi-Scale Reconstruction Of Compositional Transport

Y. Chen* (Delft University of Technology), D. Voskov (Delft University of Technology & Stanford University), M. Khait (Delft University of Technology)

Summary

The current situation with green gas emission requires the development of low carbon energy solutions. However, a significant part of the modern energy industry still relies on fossil fuels. To combine these two contradictory targets, we investigate a strategy based on a combination of CO2 sequestration with Enhanced Oil Recovery (EOR) in the hydrocarbon reservoirs. In such technology, the development of miscibility is the most attractive strategy from both technological and economic aspects. Modeling of this process involves solving complex nonlinear problem describing compositional flow and transport in highly heterogeneous porous media. An accurate capture of the miscibility development usually requires an extensive number of components to be present in the compositional problem which makes simulation run-time prohibitive for optimization. Here, we apply a multi-scale reconstructing of compositional transport to the optimization of CO2 injection. In this approach, a prolongation operator, based on the parametrization of injection and production tie-lines, is constructed following the fractional flow theory. This operator is tabulated as a function of pressure and pseudo-composition which then is used in the Operator-Based Linearization (OBL) framework for simulation. As a result, a pseudo two-component solution of the multidimensional problem will match the position of trailing and leading shocks of the original problem which helps to accurately predict phase distribution. The reconstructed multicomponent solution can be used then as an effective proxy-model mimicking the behavior of the original multicomponent system. Next, we use this proxy-model in the optimization procedure which helps to improve the performance of the process in several folds. An additional benefit of the proposed methodology is based on the fact that important technological features of CO2 injection process can be captured with lower degrees of freedom which makes the optimization solution more feasible.

Introduction

Greenhouse gas emission together with a high demand of energy has long been a concern of contemporary society. Near-miscible CO_2 injection is among the most efficient strategies for a tertiary recovery of oil (Lake, 1989); it can also reduce the carbon emission. The produced hydrocarbons can be seen as a low-carbon fuel due to the significant amount of CO_2 left in the subsurface as the result of the EOR application. Nevertheless, the heterogeneity of subsurface with complex multi-scale characteristics requires a suitable and highly resolved model to comprehend the details of flow and interactions with the subsurface.

The current economic situation, especially low oil price and formidable cost of CO_2, introduces extra challenges on applying a miscible gas injection. However, in combined objective of enhanced oil recovery and CO_2 sequestration, the development of miscibility may become the most attractive strategy from both technological and economic points of view. In addition, effective miscible injection can increase the storage capacity for CO_2 sequestration in virgin or depleted hydrocarbon fields. It is strongly recommended to develop a plausible techno-economic model to meet the combined goals of oil recovery and carbon dioxide sequestration. This serves as a primary motivation for this study.

To simulate the miscible gas injection process, compositional modeling is inevitably employed. Compositional models require numerical solution of nonlinear equations that involve mass conservation of different components and thermodynamic equilibrium. The phase behavior of multiphase multi-component mixtures is usually resolved by applying an Equation of State (EoS) (Coats, 1980). Near-miscible gas injection process usually involves a large number of species in solution, which significantly degrades simulation performance. In addition, in nonlinear iterations, thermodynamic equilibrium should be enforced in every grid block to check the phase behavior of the mixture; this adds to the performance penalty (Iranshahr et al., 2013).

Thermodynamic equilibrium usually consists of two stages: a phase stability test (Michelsen, 1982a) and flash calculation (Michelsen, 1982b). Various EoS were proposed to represent thermodynamic equilibrium in a hydrocarbon mixture, starting with the classic cubic EOS (Peng and Robinson, 1976; Soave, 1972). However, the growing accuracy of reservoir fluid characterization and better recognition of complex physical processes involving component interactions requires an application of a more complicated EOS, such as Statistical Association Fluid Theory (SAFT) (Chapman et al., 1989) or Cubic-Plus-Association (CPA) (Kontogeorgis et al., 1996). In addition, coupling with chemical reactions requires a combination of thermodynamic and chemical equilibria (Lucia et al., 2015; Paterson et al., 2018). This can significantly increase the cost of phase-behavior computations in compositional simulation (Voskov et al., 2017).

Several efforts have been made to improve the performance of the compositional reservoir simulators by improving phase-behavior computations (Voskov, 2009; Pan and Tchelepi, 2011; Iranshahr et al., 2010), spatial coarsening of compositional models (Iranshahr et al., 2014; Salehi, 2016) or reformulation of compositional nonlinear problem (Zaydullin et al., 2012). In this work, a newly proposed Multi-Scale Compositional Transport (MSCT) approach by Ganapathy (2017) is utilized for production optimization. The Algebraic Multi-Scale (AMS) approach was initially proposed to solve an elliptic flow problem by Jenny et al. (2003). Several extensions of this method have been successfully developed. However, most of the AMS methods were focused exclusively on the flow solver and did not address the transport problem, except Zhou et al. (2012), where an adaptive Multiscale Finite Volume Method was proposed to accelerate the transport solver. On the basis of these ideas, an MSCT method for reconstruction of the compositional transport problem with an arbitrary number of components was developed in Ganapathy (2017).

This approach suggests a two-stage reconstruction, where, at the first stage, the boundary of a two-phase region is recovered, and the detailed solution in the two-phase region is reconstructed in the second stage. This approach utilized an Operator-Based Linearization (OBL) technique proposed by Voskov (2017). In the OBL method, the terms of the discretized governing equations are factorized into

space- and state-dependent operators. The state-dependent operators are adaptively discretized in the parameter space of the problem, and multi-linear interpolation is applied for continuous representation (Khait and Voskov, 2017). This formulation helps to avoid the performance issues associated with an accurate phase-split evaluation and reduces the nonlinearity of the problem. Recently, this approach was extended for adaptive parametrization of thermal-compositional problems with buoyancy (Khait and Voskov, 2018).

The original study of the MSCT method was limited to isothermal two-phase flow condition with fixed phase-equilibrium ratios (K-values) (Ganapathy et al., 2018). In this work, we introduce an application of MSCT using the PR-EOS (Peng and Robinson, 1976). Due to the strong nonlinearity of the CO_2 injection system, constrained nonlinear optimization strategy is utilized to determine the optimal production scenario. For production optimization, we used only the first-stage MSCT reconstruction as a physics-based proxy model and compare its result with optimization of the full compositional solution. Both approaches were compared using an idealized conceptual model with growing optimization complexity.

Model description

In this section, a concise simulation framework based on Voskov and Tchelepi (2012) is presented.

Compositional framework

For simplicity, the thermal changes, capillarity, gravity, and diffusion are neglected in the following description. The general mass-conservation equation for component i in the two-phase compositional problem is defined as follows:

$$\frac{\partial}{\partial t}\left(\phi \sum_{j=1}^{2} x_{i,j}\rho_j S_j\right) + \nabla \cdot \sum_{j=1}^{2} x_{i,j}\rho_j \mathbf{u_j} + \sum_{j=1}^{2} x_{i,j}\rho_j q_j = 0, \quad i = 1,...,N_c \tag{1}$$

In eq. (1), t is time, ϕ is the porosity of the reservoir, ρ_j is molar phase density, S_j is phase saturation,$x_{i,j}$ is the mole fraction of component i in phase j, q_j is the source or sink term of phase j, and N_c is number of the components. The Darcy velocity $\mathbf{u_j}$ is defined as

$$\mathbf{u_j} = -K\frac{k_{rj}}{\mu_j} \cdot \nabla p, \quad j = 1,2, \tag{2}$$

where K is absolute permeability, k_{rj} is the relative permeability of phase j, μ_j is viscosity of phase j and p is pressure. The equilibrium relations between oil and gas phase are required to close the system

$$\hat{f_{i,o}}(p,T,\mathbf{x_o}) = \hat{f_{i,g}}(p,T,\mathbf{x_g}), \quad i = 1,...,N_c, \tag{3}$$

where $\hat{f_{i,o}}$ and $\hat{f_{i,g}}$ are the fugacities for the component i in oil phase and gas phase, respectively. Fugacity is a function of pressure (p), temperature (T) and phase compositions ($x_{i,j}$), which are determined by EoS-based flash computations. Additional equations are given as follows to close the system of governing equations:

$$\sum_{i=1}^{N_c}(x_{i,1} - x_{i,2}) = 0, \quad i = 1,...,N_c, \tag{4}$$

$$s_o + s_g = 1. \tag{5}$$

The overall composition of i component can be expressed as:

$$z_i = \sum_{j=1}^{2} v_j x_{i,j}, \quad i = 1,...,N_c, \tag{6}$$

where, v_j is the molar fraction of the phase $j(o,g)$. Solving the eqs. (3) to (6) is a procedure called multiphase flash (Michelsen, 1982b), which will provides phase composition $x_{i,j}$ and phase fraction v_j.

Finally, the phase saturation s_j can be found from

$$s_g = \frac{v_g}{\rho_g} / (\frac{v_g}{\rho_g} + \frac{v_o}{\rho_o}) \tag{7}$$

Applying two-point finite-volume in space and backward Euler in time discretizations, the general mass-conservation equation is written as:

$$V\left(\left(\phi\sum_{j=1}^{2}x_{i,j}\rho_j S_j\right)^{n+1}-\left(\phi\sum_{j=1}^{2}x_{i,j}\rho_j S_j\right)^{n}\right)-\Delta t\sum_{l\in\mathbf{L}}\left(\sum_{j=1}^{2}x_{i,j}^{l}\rho_j^{l}T_j^{l}\Delta\Psi^{l}\right)+V\Delta t\sum_{j=1}^{2}x_{i,j}\rho_j q_j=0, \tag{8}$$

where V is total control volume and $\mathbf{L}$ represents the interface which connects the control volume with another grid blocks. In the simplified assumptions, mentioned above, $\Delta\Psi^l$ becomes a pressure difference between two connected grid blocks. Finally, T_j^l is the transmissibility of phase j.

Operator-Based Linearization

The multi-scale technique is implemented on the basis of an Operator-based Linearization (OBL) approach proposed by Voskov (2017). To apply OBL, the discretized mass conservation equation (eq. (8)) is written in the following residual form:

$$R_i(\xi,\omega,\mathbf{u}) = a(\xi)\left(\alpha_i(\omega)-\alpha_i(\omega_n)\right)-\sum_{\nu}\beta_i^{\nu}(\omega)b^{\nu}(\xi,\omega)+\theta_i(\xi,\omega,\mathbf{u})=0. \tag{9}$$

The operators in eq. (9) are defined as follows:

$$\alpha_i(\omega) = (1+c_r(p-p_{ref}))\sum_{j=1}^{2}x_{i,j}\rho_j S_j, \tag{10}$$

$$a(\xi) = V(\xi)\phi_0(\xi), \tag{11}$$

$$\beta_i(\omega) = \sum_{j}^{2}x_{i,j}\frac{k_{rj}}{\mu_j}\rho_j, \tag{12}$$

$$b(\xi,\omega) = \Delta t T_{ab}(\xi)(p^b-p^a), \tag{13}$$

$$\theta_i(\xi,\omega,\mathbf{u}) = \Delta t\sum_{j=1}^{2}x_{i,j}\rho_j q_j(\xi,\omega,\mathbf{u}). \tag{14}$$

In eq.(10) to eq.(14), c_r is rock compressibility and T^{ab} is the transmissibility between grid-blocks. The vector $\mathbf{u}$ contains well-control variables, ω is the set of state variables and ξ are the set of spatial coordinates. In addition, α_i is the accumulation operator, β_i is the flux operator and θ_i is the source/sink operator. The OBL approach is based on a simplified representation of the nonlinear operators in the parameter space of the simulation problem. For an isothermal reservoir simulation, the parameter space is defined by the range of pressure (p) between injection and production conditions and overall compositional (z_i) range from 0 to 1. The fully implicit method (FIM) is utilized to resolve the given governing equation eq. (9) based on the unknowns set. The eq. (9) to eq.(14) represent a full conventional compositional model.

Multi-Scale Compositional Transport

A solution of a compositional transport problem can be shown in a phase diagram by the solution path in compositional space, which defines the compositional changes between the initial and injection mixtures. Conservation principles and fractional-flow theory form the foundation for the general solution

method (Orr, 2007). The compositional path of the conventional compositional problem for gas injection process always results in two shocks (leading and trailing shocks) between single- and two-phase regions. In a ternary diagram (Fig. 1a), it is presented as yellow lines connecting the initial oil and injected gas composition.

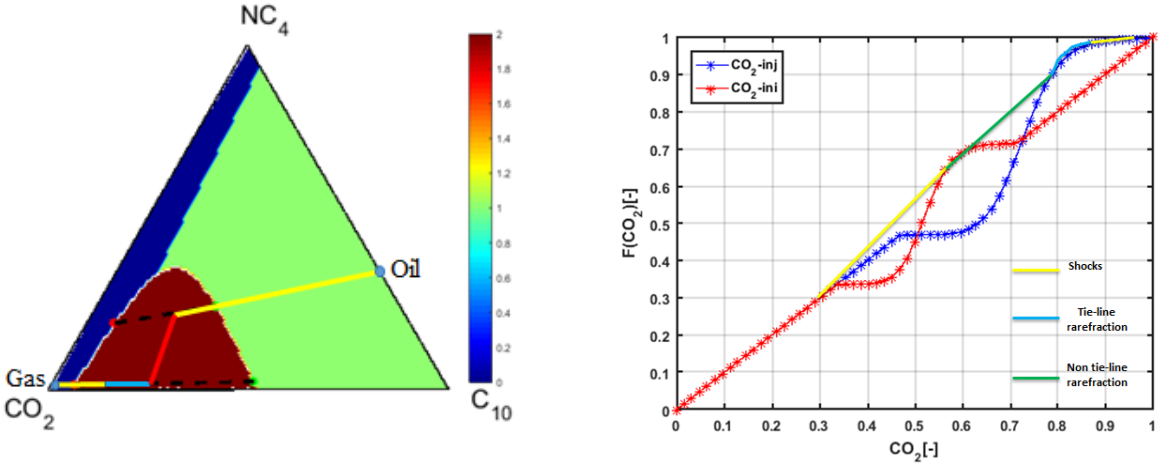

(a) *(b)*

Figure 1 *Gas-injection solution in ternary system: (a) ternary diagram with displacement path and two key tie-lines and (b) fractional-flow curves for component CO_2 with solution path.*

The shocks between single- and two-phase regions are always aligned along two key tie-lines (black dashed lines) defined by liquid x_i and vapor y_i fractions of each component. For a fixed pressure, x_i and y_i remain constant and it is possible to construct the fractional-flow curve corresponding with compositional transport, see eq. (15). Fig. 1b gives the injection and initial fractional-flow curves for CO_2 in a ternary system corresponding to the injection and initial tie lines in Fig. 1a.

$$F_i = x_i(1-f_g) + y_i f_g, \quad i = 1,...,N_c - 1 \tag{15}$$

The proposed Multi-Scale Compositional Transport approach consists of two stages (Ganapathy et al., 2018). The first stage utilizes the set of restriction-prolongation operators for reconstructing two-phase boundaries (the trailing and leading shocks). The restriction here reduces the $n_c - 1$ transport equations to a single equation with a special flux operator based on the pseudo-fractional-flow curve. In the second stage, the set of restriction-prolongation operators is applied in the two-phase region to reconstruct the solution structure of the two-phase displacement. This stage is based on the invariance of two-phase solutions in tie-line space reported in Voskov and Entov (2001) and adapted for practice in Voskov and Tchelepi (2009).

The proxy model for compositional simulation, utilized in this work, uses the first-stage multi-scale reconstruction from Ganapathy et al. (2018). A restriction operator combines two fractional-flow curves for injection and production tie-lines, defined as:

$$F_I^{ini} = x_I^{ini}(1-f_g) + y_I^{ini} f_g, \quad F_I^{inj} = x_I^{inj}(1-f_g) + y_I^{inj} f_g. \tag{16}$$

The equivalent fractional-flow curve, serving as the restriction operator, is constructed by taking a convex hull on the union of both curves:

$$F_R = \mathrm{conv}(F_I^{inj} \cup F_I^{ini}) \tag{17}$$

In Fig. 2, this curve is shown in green. Next, the equivalent values of F_i and z_i from the green curve are tabulated into the restriction operator and the reduced system is solved. The reduced system of

equations includes the convenient pressure equation and the restricted transport equation based on the constructed pseudo-fractional-flow curve. In structure, this system is very close to the conventional binary compositional problem. Fig. 3 gives an example of the operators which are tabulated from the

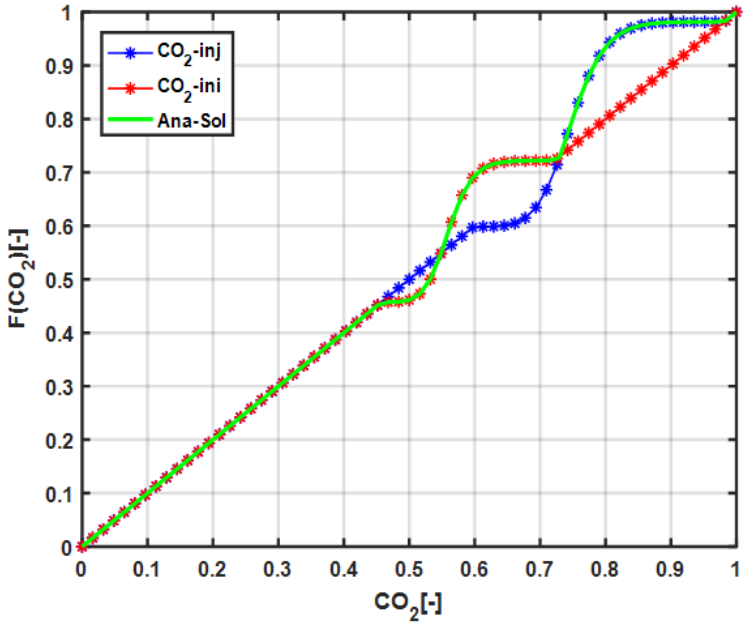

Figure 2 *Analytical fractional flow for CO_2.*

analytical fractional flow curve. Those operators are utilized in the OBL framework (Khait and Voskov, 2017) to solve the first-stage restricted system.

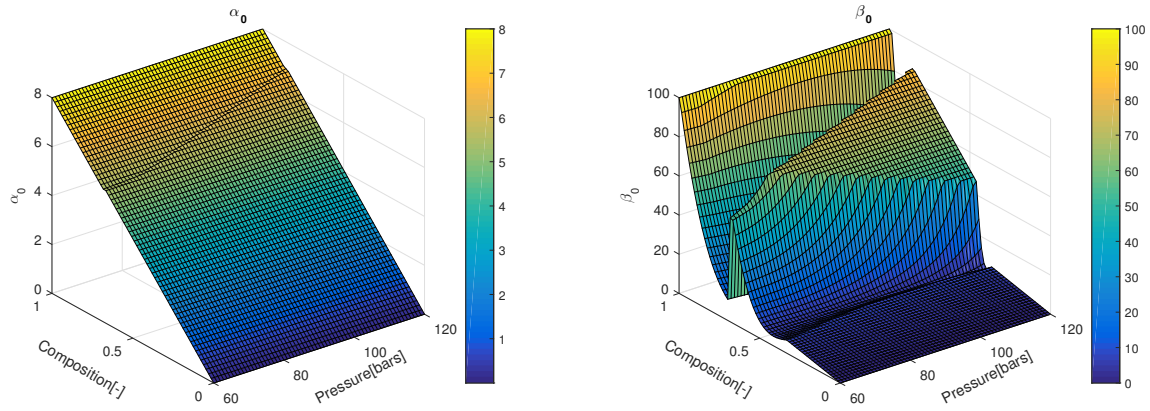

(a) ***(b)***

Figure 3 *Operators for a restricted compositional system parameterized at N=64.*

Once the solution of the restricted system is found, the full system is reconstructed based on the prolongation operator. This operator applies interpolation between initial and injection compositions using the solution of the restricted system $\boldsymbol{\kappa}(z_R)$ as an indicator:

$$\boldsymbol{\kappa}(z_R)\left[\mathbb{R}^1 \Longrightarrow \mathbb{R}^{n_c-1}\right] : \mathbf{z} = \mathbf{I}_{\{z^{ini},z^{inj}\}}(z_R). \tag{18}$$

Here, $\boldsymbol{\kappa}$ is the interpolation-prolongation operator, z_R is the restricted solution and $\mathbf{I}$ is the piecewise linear interpolation function. Referring to this linear interpolation, the transport solution of other components in the multicomponent system is reconstructed and used as a proxy model in place of the full

compositional model. Notice that this system can accurately predict only the boundaries of the two-phase region and their dynamic propagation in space; for a really accurate solution, the second-stage multi-scale reconstruction should be applied (Ganapathy et al., 2018).

Economic model

The techno-economic model is applied to evaluate the economics of a combined CO_2 EOR and sequestration application. Several economic studies of CO_2 injection processes have been performed by Tayari et al. (2018); Kwak and Kim (2017); Ettehadtavakkol et al. (2014); Rubin et al. (2007). McCoy and Rubin (2009) proposed several regression equations for assessment of the capital cost of CO_2 injection projects, which are validated by Wei et al. (2015) and Ettehadtavakkol et al. (2014). Referring to Tayari et al. (2018), this techno-economic model uses simulation input data and oil production rate, gas injection rate and Bottom-Hole Pressure (BHP) to define different costs and revenues of the project.

On the basis of reservoir-simulation data, an economic model is developed to estimate the profitability of CO_2 injection for Enhanced Oil Recovery (EOR) and CO_2 sequestration, which will reflect on the Net Present Value (NPV). The general economic parameters of a CO_2 injection process are listed in Fig. 4. This figure shows that the cost of a CO_2 injection project can be divided into two parts, which are capital

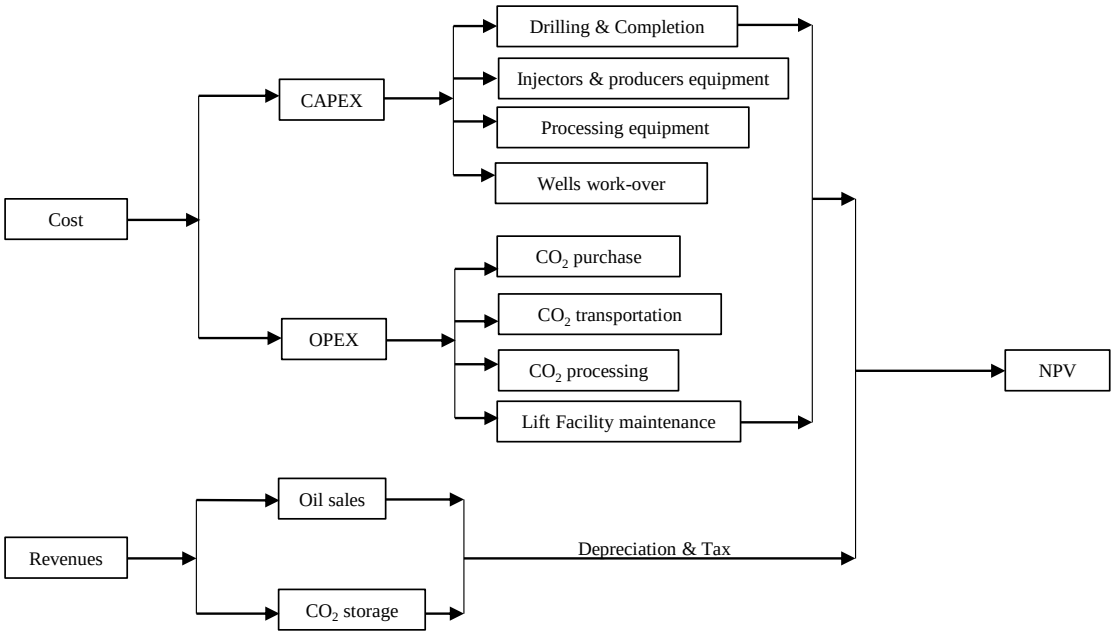

Figure 4 *General economic parameters for CO_2 injection project.*

cost and operational cost. Dominant revenues from the gas-injection project mainly originate from oil sales and carbon sequestration incentives. A previous economic study of CO_2-injection projects (Kwak and Kim, 2017) indicates that CO_2 purchasing cost is one of the most sensitive parameters when NPV is evaluated. In this work, according to the general parameters and equations provided in Kwak and Kim (2017), a spider plot is constructed in Fig. 5, which shows that CO_2 processing cost has a similar impact on NPV as CO_2 purchasing cost. The CO_2 processing-cost model in this work is based on Tayari et al. (2018), and is expressed in terms of the pump capital cost as follows:

$$C_{pump} = \left(1.35 \times 10^3 \times W_p\right) + 0.085 \times 10^6, \tag{19}$$

where W_p is pumping power requirement, which is expressed in kW, which in turn varies with CO_2 injection pressure. Other parameters in the economic model are listed in Table 1. Some of them are obtained by introducing the regression equations listed in McCoy and Rubin (2009), such as those for well engineering cost and CO_2 processing equipment cost.

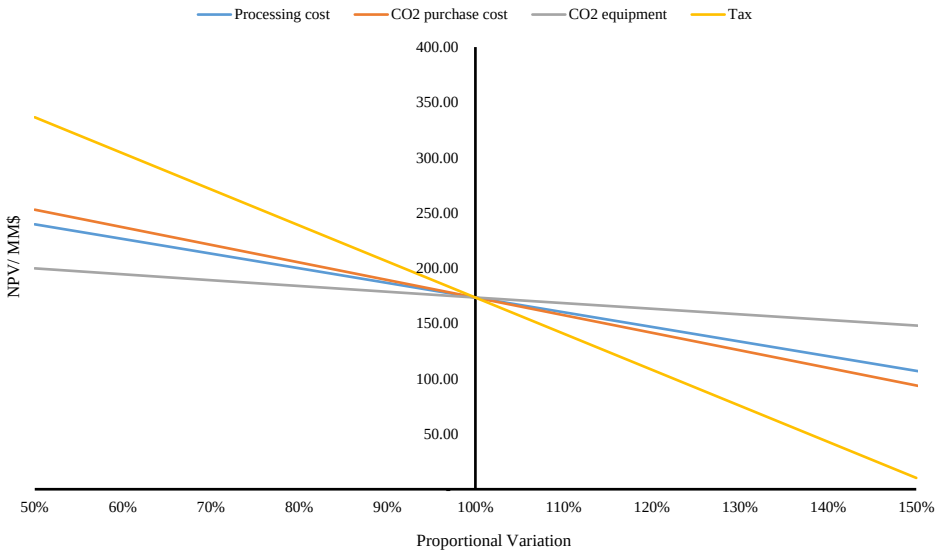

Figure 5 *General sensitivity study for Net Present Value (NPV).*

Table 1 *The values for economic parameters.*

Parameters		Units	Remarks
CO_2 storage incentives	12	\$/t	Kwak and Kim (2017)
Well engineering cost	501644	\$	McCoy and Rubin (2009)
CO_2 processing equipment	10637265	\$	McCoy and Rubin (2009)
Wells work-over	241429	\$	McCoy and Rubin (2009)
CO_2 purchase cost	24	\$/t	Kwak and Kim (2017)
CO_2 transportation	0	\$/t	CO_2 source in-situ
CO_2 processing cost	10	\$/t	Rubin et al. (2007)
Lift facility maintenance	0.6	\$/t	Rubin et al. (2007)
CO_2 net cost	12	\$/t	Purchasing cost-Incentives
Tax rate(royalty, severance tax)	0.4	[-]	McCoy and Rubin (2009)
Depreciation	Linear over ten years	\$	
Discount rate	12	[-]	Wei et al. (2015)

Numerical results

In this section, we demonstrate the comparison between solutions of the proxy model and the full compositional model. Here, we limit our investigation to a conceptual 1D reservoir model for simplicity. In this model, the injection well on the left operates at a constant gas rate when the production well is controlled by Bottom-Hole Pressure (BHP) which serves as a control variable for optimization.

Restricted solution

Fig. 6 shows the restricted solution z_R, which yields the shock reconstruction curves for simulation results for the growing BHP at the production well. All simulation results are shown for the model with parameters specified in Appendix A after 1000 days of simulation. The K-value table in this work is obtained from the embedded Constant Composition Expansion (CCE) experiments in Geoquest (2008) based on the PR EoS, which is shown in Tab 7. It is clear that the K-value system does not develop miscibility even when BHP provides the pressure at the displacement front close to the First-Contact Minimal Miscibility Pressure (FC MMP) for this system (around 126 bars at T = 373K). This happens due to the inability of the K-value model to predict miscibility accurately, since compositional dependency is not captured in this model.

It can be overcome by either extension of the K-value parameterization with additional degrees of freedom (e.g. Rannou et al., 2013) or incorporation of EoS-based phase behavior (Voskov and Tchelepi, 2009). However, it is clear that the two-phase boundaries can be accurately represented by the restricted model for K-value based physics. In addition, the complexity and structure of the restricted solution are invariant with respect to the number of components present and only depends on initial and injection tie-lines in the multi-component system (see Ganapathy et al., 2018, for details).

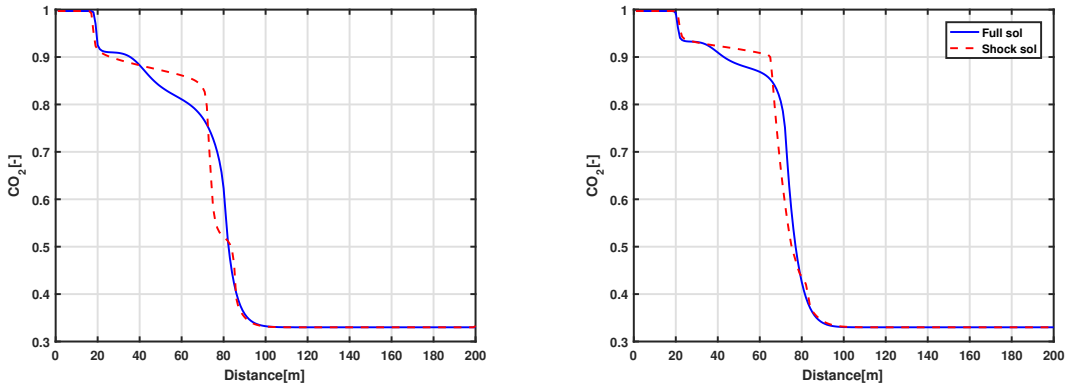

(a) *Restricted solution for BHP = 85 bars* ***(b)*** *Restricted solution for BHP= 120 bars*

Figure 6 *Shock reconstruction of the four-component system for two different BHP controls at production well (K-values).*

Next, the results of the restricted solution for the compositional problem based on the EOS is shown. The structure of the compositional transport solution depends on key tie-lines (Orr, 2007). For the restricted solution, we follow the same strategy as before and construct the restriction operator based on combined fractional flow (eq. (16)) according to the first stage of MSCT approach (Ganapathy et al., 2018). The solution of the restricted transport equation reconstructs the boundaries of the two-phase region using one transport equation instead of $n_c - 1$ equations in the conventional compositional model.

The results of quaternary system reconstruction are shown in Fig. 7. Here you can see that for a high BHP value, the structure of the solution is much closer to miscibility (leading and trailing shocks stays closer to each other) than in the K-value approximation. This happens because the EOS-based phase behavior correctly represents the compositional dependency of the solution. Similar to the K-value model, the restriction stage requires the solution of only one equation instead of $n_c - 1$, where n_c is the number of components.

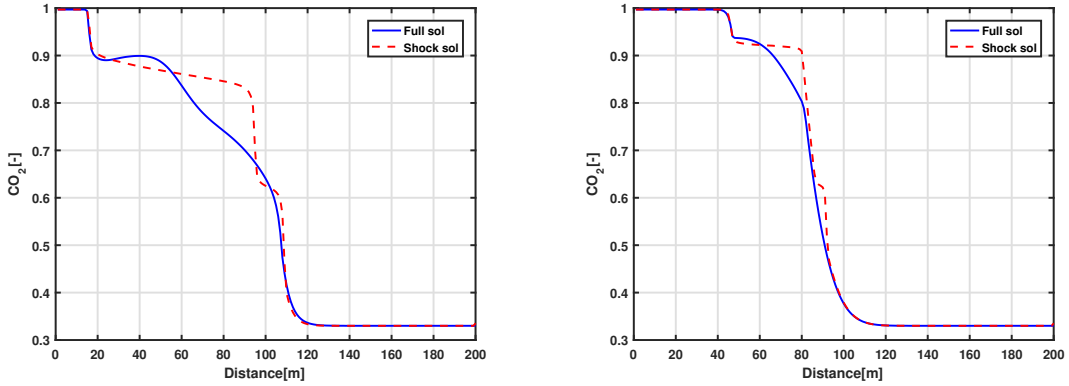

(a) *Restricted solution for BHP = 85 bars* ***(b)*** *Restricted solution for BHP = 120 bars*

Figure 7 *Shock reconstruction of the four-component system for two different BHP controls at production well (EoS model).*

Prolongation of proxy model

Here, we illustrate the construction of the proxy model using an interpolation-based prolongation operator (eq. (18)) for both cases. It can be seen in Fig. 8 and Fig. 9 that the prolongation operator does not reconstruct the full structure of the solution, but only one indicator component. For the full solution, the second stage of the reconstruction should be applied; see Ganapathy et al. (2018) for details. However, the prolongation yields a full compositional solution in every control volume, which then can be used in a multiphase flash procedure to predict phase behavior. This phase behavior provides the boundary of the two-phase region in space. In our proxy model, we are using this prediction to compute phase rates at wells and evaluate NPV for the proxy model.

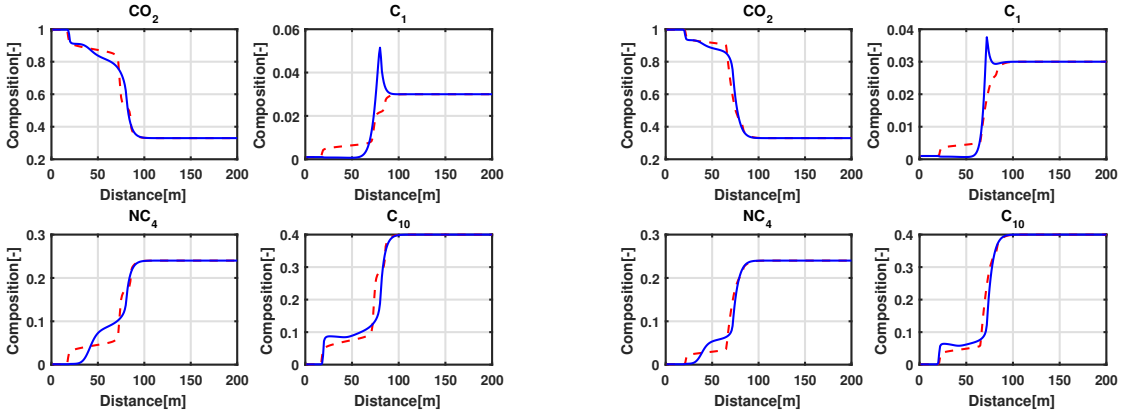

(a) *Full solution for BHP = 85 bars* ***(b)*** *Full solution for BHP = 120 bars*

Figure 8: *Proxy model for a four-component system (K-value based)*

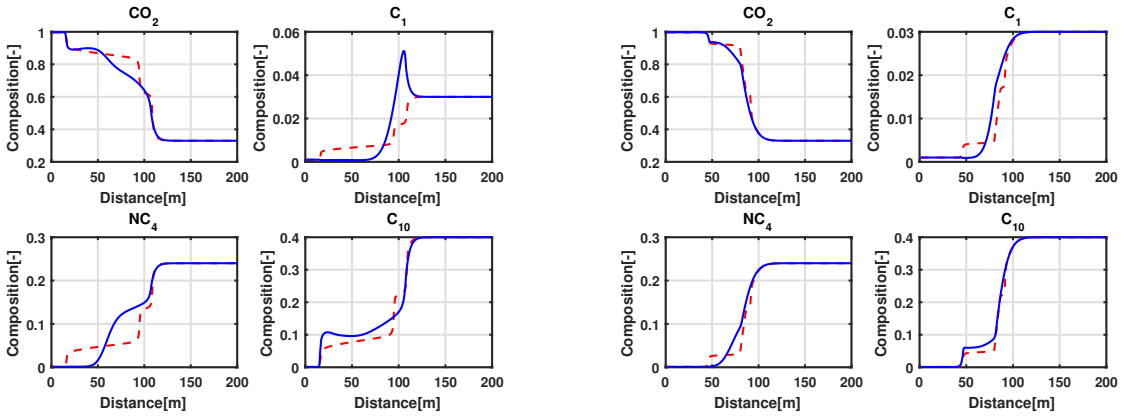

(a) *Full solution for BHP = 85 bars* ***(b)*** *Full solution for BHP = 120 bars*

Figure 9 *Proxy model for a four-component system (EoS based).*

Conceptual optimization problem

Fig. 10 shows the transport solution for both fully compositional and proxy models for different BHP controls at the production well and a fixed rate at the gas-injection well. It is clear that with increasing pressure, both models capture the development of miscibility, with the leading and trailing shocks getting closer to each other and the displacement efficiency growing. Next, we investigate optimal production strategies for this model.

In the optimization stage, the full four-component system together with the proxy two-component system is used to determine oil production. Net Present Value (NPV) is used as an indicator to estimate the economic profitability of the project. The simulation time is divided into several periods where changes

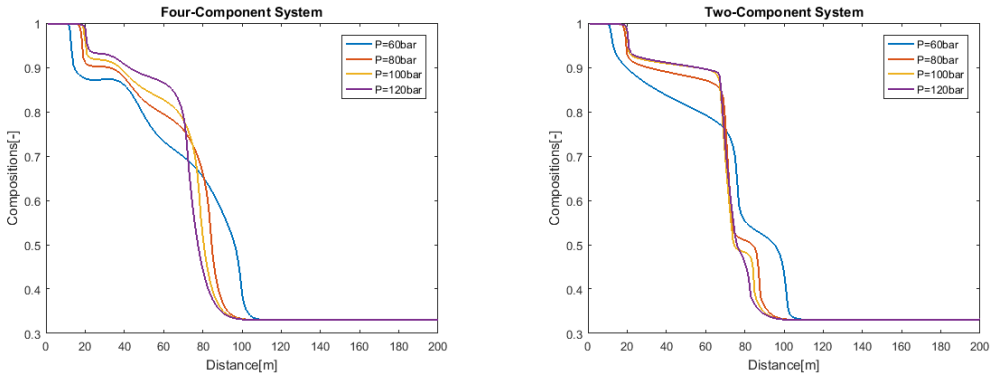

(a) *Four-component system (T = 1000days)* ***(b)*** *Two-component system(T = 1000days)*

Figure 10 *Transport solution and pressure profile for five different BHP controls at the producer.*

in BHP at production well are applied. Here we make sure that the time period for simulation covers the breakthrough of the trailing shock at the lower limit of pressure. Next, we estimate the optimal production strategy with a different numbers of control variables.

NPV with a limited number of control parameters

The NPV distribution as a function of a single BHP control is evaluated here. We compare the NPV curve vs. BHP control for both the proxy and the full compositional model. The simulation time is defined to be long enough for the breakthrough of both leading and trailing shocks of the solution. NPV plot as a function of control BHP is shown in Fig. 11. Here, the green solid curve is the NPV results

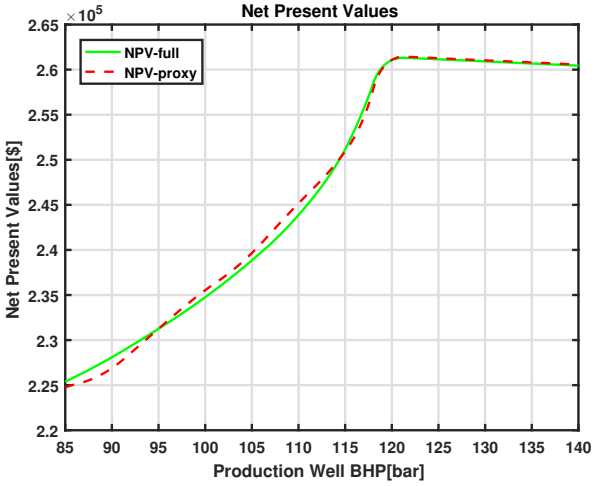

Figure 11: *NPV with one control parameter*

from the full four-component model, and red dashed curve is the NPV results from the proxy model. While there are some discrepancies in the proxy solution due to the limited application of the MSCT (only first stage of reconstruction), the model captures the correct boundaries of the two-phase region and yields the correct maximum of the NPV function. To reduce the differences in NPV evaluation, the second stage of the MSCT reconstruction can always be performed.

Next, we introduce two simulation time periods and two control variables (BHP_1 and BHP_2) for NPV evaluation. Performing an exhaustive search in the space of control variables, we evaluate the NPV function, shown in Fig. 12. While the NPV function is different for the proxy and the full model, the maximum NPV is reached at the same control values, i.e. around $BHP_1 = 95$ bars and $BHP_2 = 118$ bars. These values are conditioned by the obvious strategy for production controls when in the first time

interval, the lower BHP at the production well provides the near-miscible pressure at the displacement front. In the second time interval, the higher pressure at the production well provides near-miscible pressure until the breakthrough to the production well. The near-miscible strategy is optimal since it maximizes the oil recovery and sequestration of CO_2.

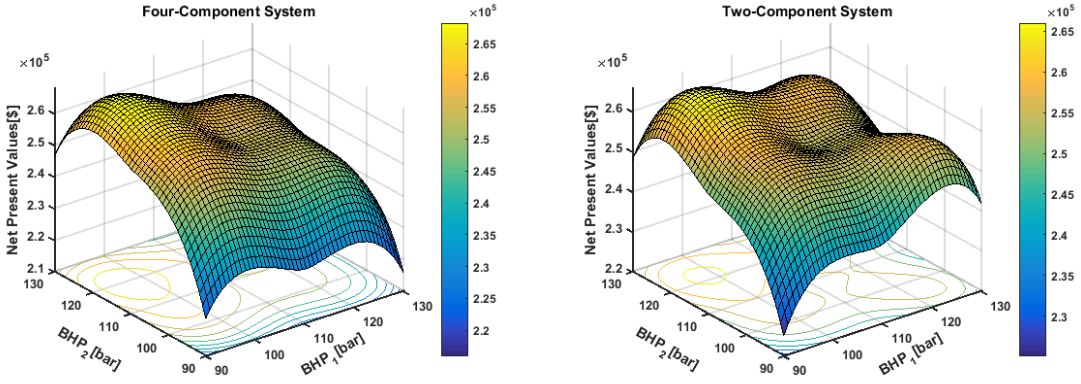

(a) *Full model* ***(b)*** *Proxy model*

Figure 12 *NPV with two control parameters.*

Optimization with multiple controls

Next, we apply production optimization based on five control variables (BHP's) corresponding to five time periods in the simulation. In this study, we use the 'fmincon' function from the Matlab optimization toolbox (MathWorks, 2018). In 'fmincon', the 'sqp' algorithm has been chosen. The optimizer is utilized to provide BHP controls at each time period and obtain an optimal NPV result during the CO_2-injection process. All BHP controls were bounded by $\text{BHP}_{min} = 60$ bars and $\text{BHP}_{max} = 140$ bars. Note, that the expected optimal strategy should include a gradual increase of BHP at each consecutive control interval to provide near-miscible conditions at the displacement front.

We test several initial guesses for the optimization with five control parameters. For this number of controls, several local minima can exist and the optimizer struggles with finding a single global extremum. However, based on the structure of solution in Fig. 10, we can predict a near-optimal BHP strategy where BHP should monotonically increase with time to provide the near-miscible pressure at the displacement front. Using this strategy with BHP = $[63; 77; 83; 102; 121]$ at five controls intervals as the initial guess, we perform the optimization. The results of optimization based on the full and proxy models are present in Table 2. You can see that the proxy model performed fewer iterations and obtained a similar NPV.

In addition, we perform two more optimization runs with different initial guesses when all BHP controls have been set to 70 bars and 100 bars respectively. The results can also be seen in Table 2. In these optimization runs, both models cannot converge to the same optimal strategy, but getting close to it. The proxy model performs quite robustly and proves to be applicable for optimization of gas injection process in the idealistic reservoir.

Conclusion

In this work, we extend the Multi-Scale Compositional Transport (MSCT) approach for the EoS-based gas-injection problems. In particular, we parametrize the restriction operator of the first stage MSCT reconstruction in the pressure interval and obtain the restricted solution using the Operator-Based Linearization framework. The restricted solution was prolongated to the full compositional solution using interpolation operator. The obtained proxy model can accurately predict the boundaries of the two-phase region and has been utilized in this work for production optimization.

Referring to previous economic assessments of CO_2-injection projects, a techno-economic model has

Table 2 *Optimization results for constant initial BHP.*

Initial guess	Model	# of iter.	NPV($)	Controls for time periods				
				1	2	3	4	5
Near optimal	Full model	6	261,100	60.00	76.18	79.21	88.21	117.65
	Proxy model	3	261,064	60.00	76.08	80.07	85.00	117.99
BHP = 70 bars	Full model	11	261,007	60.00	79.33	90.76	63.02	126.11
	Proxy model	12	260,247	60.97	60.05	89.62	117.41	127.74
BHP = 100 bars	Full model	9	260,093	60.00	87.86	107.42	82.86	121.16
	Proxy model	7	260,817	60.00	95.05	105.73	61.97	118.87

been developed to analyze the revenues of CO_2 injection for the combined objective of EOR and sequestration. We demonstrate that the objective function of full compositional model and the proposed proxy model share the same extrema for a limited number of control parameters. In addition, a constrained nonlinear optimization is applied to determine an optimal production strategy for the gas injection operation. Both models converge to a similar optimal strategy when the initial guess is close to the optimal solution. For arbitrary initial guesses, the converged optimal strategy may differ for proxy and full compositional models. In our future work, we will extend the proposed methodology to more realistic 3D simulation problems.

Acknowledgements

We acknowledge financial support from Xodus Group. We also would like to acknowledge the technical assistance by Mark Khait during this study.

References

Chapman, W., Gubbins, K., Jackson, G. and Radosz, M. [1989] SAFT: Equation-of-state solution model for associating fluids. *Fluid Phase Equilibria*, **52**, 31 – 38.

Coats, K.H. [1980] An Equation of State Compositional Model. *SPE Journal*, **20**(05), 363–376.

Ettehadtavakkol, A., Lake, L.W. and Bryant, S.L. [2014] CO2-EOR and storage design optimization. *International Journal of Greenhouse Gas Control*, **25**, 79 – 92.

Ganapathy, C. [2017] *Multiscale Reconstruction of Compositional Transport*. Master's thesis, Delft University of Technology.

Ganapathy, C., Chen, Y. and Voskov, D. [2018] Multiscale Reconstruction of Compositional Transport. In: *ECMOR 2018-16th European Conference on the Mathematics of Oil Recovery*.

Geoquest [2008] *PVTi Reference Manual*. Schlumberger.

Iranshahr, A., Chen, Y. and Voskov, D.V. [2014] A coarse-scale compositional model. *Computational Geosciences*, **18**(5), 797–815.

Iranshahr, A., Voskov, D. and Tchelepi, H. [2010] Generalized negative flash method for multiphase muticomponent systems. *Fluid Phase Equilibria,*, **299**, 272–283.

Iranshahr, A., Voskov, D. and Tchelepi, H. [2013] A negative-flash tie-simplex approach for multiphase reservoir simulation. *SPE Journal*, **18**(6), 1140–1149.

Jenny, P., Lee, S.H. and Tchelepi, H.A. [2003] Multi-scale Finite-volume Method for Elliptic Problems in Subsurface Flow Simulation. *J. Comput. Phys.*, **187**(1), 47–67.

Khait, M. and Voskov, D. [2018] Adaptive Parameterization for Solving of Thermal/Compositional Nonlinear Flow and Transport With Buoyancy. *SPE Journal*, **33**(02), 522 – 534. SPE-182685-PA.

Khait, M. and Voskov, D.V. [2017] Operator-based linearization for general purpose reservoir simulation. *Journal of Petroleum Science and Engineering*, **157**, 990 – 998.

Kontogeorgis, G.M., Voutsas, E.C., Yakoumis, I.V. and Tassios, D.P. [1996] An Equation of State for Associating Fluids. *Industrial & Engineering Chemistry Research*, **35**(11), 4310–4318.

Kwak, D.H. and Kim, J.K. [2017] Techno-economic evaluation of CO2 enhanced oil recovery (EOR) with the optimization of CO2 supply. *International Journal of Greenhouse Gas Control*, **58**, 169 – 184.

Lake, L.W. [1989] *Enhanced oil recovery*. Prentice-Hall.
Lucia, A., Henley, H. and Thomas, E. [2015] Multiphase equilibrium flash with salt precipitation in systems with multiple salts. *Chemical Engineering Research and Design*, **93**, 662–674.
MathWorks [2018] MATLAB Optimization Toolbox.
McCoy, S.T. and Rubin, E.S. [2009] The effect of high oil prices on EOR project economics. *Energy Procedia*, **1**(1), 4143 – 4150. Greenhouse Gas Control Technologies 9.
Michelsen, M.L. [1982a] The isothermal flash problem. Part I. Stability. *Fluid Phase Equilibria*, **9**(1), 1 – 19.
Michelsen, M.L. [1982b] The isothermal flash problem. Part II. Phase-split calculation. *Fluid Phase Equilibria*, **9**(1), 21 – 40.
Orr, F.M. [2007] *Theory of Gas Injection Process*. Tie-Line Publications, Denmark:Holte.
Pan, H. and Tchelepi, H.A. [2011] Compositional Flow Simulation Using Reduced-Variables and Stability-Analysis Bypassing. In: *SPE Reservoir Simulation Symposium*. SPE-142189-MS.
Paterson, D., Michelsen, M., Yan, W. and Stenby, E. [2018] Extension of modified RAND to multiphase flash specifications based on state functions other than (T,P). *Fluid Phase Equilibria*, **458**, 288–299.
Peaceman, D.W. [1978] Interpretation of Well-Block Pressures in Numerical Reservoir Simulation. *SPE Journal*, **18**(03), 183 – 194. SPE-6893-PA.
Peng, D.Y. and Robinson, D.B. [1976] A New Two-Constant Equation of State. *Industrial & Engineering Chemistry Fundamentals*, **15**(1), 59–64.
Rannou, G., Voskov, D. and Tchelepi, H. [2013] Tie-line-based K-value method for compositional simulation. *SPE Journal*, **18**(6), 1112–1122.
Rubin, E.S., Chen, C. and Rao, A.B. [2007] Cost and performance of fossil fuel power plants with CO2 capture and storage. *Energy Policy*, **35**(9), 4444 – 4454.
Salehi, A. [2016] *Upscaling of Compositional Flow Simulation Based on a Non-Equilibrium Formulation*. Ph.D. thesis, Stanford University.
Soave, G. [1972] Equilibrium constants from a modified Redlich-Kwong equation of state. *Chemical Engineering Science*, **27**(6), 1197 – 1203.
Tayari, F., Blumsack, S., Johns, R.T., Tham, S. and Ghosh, S. [2018] Techno-economic assessment of reservoir heterogeneity and permeability variation on economic value of enhanced oil recovery by gas and foam flooding. *Journal of Petroleum Science and Engineering*, **166**, 913 – 923.
Voskov, D. and Entov, V. [2001] Problem of oil displacement by gas mixtures. *Fluid Dynamics*, **36**(2), 269–278.
Voskov, D., Henley, H. and Lucia, A. [2017] Fully compositional multi-scale reservoir simulation of various CO2 sequestration mechanisms. *Computers and Chemical Engineering*, **96**, 183–195.
Voskov, D. and Tchelepi, H. [2009] Compositional space parameterization: Theory and Application for Immiscible Displacements. *SPE Journal*, **14**(03), 431–440.
Voskov, D.V. [2017] Operator based linearization approach for modeling of multiphase multicomponent flow in porous media. *Journal of Computational Physics*, **337**, 275 – 288.
Voskov, D.V. and Tchelepi, H.A. [2012] Comparison of nonlinear formulations for two-phase multi-component EoS based simulation. *Journal of Petroleum Science and Engineering*, **82-83**, 101 – 111.
Voskov, D. V.and Tchelepi, H.A. [2009] Compositional Space Parameterization: Multicontact Miscible Displacements and Extension to Multiple Phases. *SPE Journal*, **14**(03), 441–449. SPE-113492-PA.
Wei, N., Li, X., Dahowski, R.T., Davidson, C.L., Liu, S. and Zha, Y. [2015] Economic evaluation on CO2-EOR of onshore oil fields in China. *International Journal of Greenhouse Gas Control*, **37**, 170 – 181.
Zaydullin, R., Voskov, D. and Tchelepi, H.A. [2012] Nonlinear Formulation Based on an Equation-of-State Free Method for Compositional Flow Simulation. Society of Petroleum. *SPE Journal*, **18**(02), 264–273. SPE-146989-PA.
Zhou, H., Lee, S.H. and Tchelepi, H.A. [2012] Multiscale Finite-Volume Formulation for Saturation Equations. *SPE Journal*, **17**(01), 198 – 211. SPE-119183-PA.

Appendix A: Fluid and rock interactions

The simulation model in this study is a 1D homogeneous model ($K = 20$ mD), 200 m long with one injection well on the left and one production well on the right boundaries. The finite volume discretization

is applied based on the standard Cartesian grid with the block sizes: Δx = 1m, Δy = 10m, Δz = 1m. For the well model, the Peaceman formula (Peaceman, 1978) is utilized with $r_w = 0.15$ m. The injection well is controlled by a constant gas rate $q_g = 2m^3/day$. The rest of parameters are specified in tables below.

Table 3 *Hydrodynamic parameters.*

Phase	Oil	Gas
Rock compressibility, 1/bar	10^{-5}	
Porosity	0.3	
Residual saturation (S_{jr})	0.0	0.0
End point relative permeability (K_{rje})	1.0	1.0
Saturation exponent (n_j)	2.0	2.0
Viscosity, cP (μ_j)	0.5	0.1

Table 4: *Thermodynamic properties.*

Components	CO_2	C_1	C_4	C_{10}
Critical pressure, bars	73.87	43.04	37.47	24.20
Critical temperature, K	304.7	190.60	419.5	626.0
Critical volume, m^3 / kg-mole	0.094	0.098	0.258	0.534
Acentric factor	0.225	0.013	0.1956	0.385
Molar weight, g/mol	44.01	16.04	58.12	134.0
Binary interaction, CO_2	-	0.1	0.1	0.1
Binary interaction, C_1	0.1	-	-	0.041

Table 5: *Binary system.*

	Binary system	
Compositions	CO_2	C_{10}
Initial Oil Compositions	0.33	0.67
Injection gas Compositions	1.00	0.00

Table 6: *Quaternary system.*

	Quaternary system			
Compositions	CO_2	C_1	NC_4	C_{10}
Initial Oil Compositions	0.33	0.03	0.24	0.40
Injection gas Compositions	1.00	0.00	0.00	0.00

For the K-value model, we perform the Constant Composition Expansion (CCE) using PVTi module (Geoquest, 2008) where we generate K-value table corresponding to given initial compositions in Tab. 6. The K-value table is present as a function of pressure with three pressure values employed, see Tab. 7 for details.

Table 7 *K-value table for quaternary system.*

Pressure	Compositions			
	CO_2	C_1	NC_4	C_{10}
40 bars	6.70	8.60	1.20	0.00085
80 bars	2.05	4.70	0.54	0.005
120 bars	1.33	2.51	0.31	0.09